Direct proton decay of the isoscalar giant dipole resonance

Hunyadi, M; van den Berg, AM; Blasi, N; Baumer, C; Csatlos, M; Csige, L; Davids, B; Garg, U; Gulyas, J; Harakeh, MN

Published in:
Physics Letters B

DOI:
10.1016/j.physletb.2003.10.016

Available online at www.sciencedirect.com
SCIENCE DIRECT®

PHYSICS LETTERS B

Physics Letters B 576 (2003) 253–259

www.elsevier.com/locate/physletb

Direct proton decay of the isoscalar giant dipole resonance

M. Hunyadi [a,1], A.M. van den Berg [a], N. Blasi [b], C. Bäumer [c], M. Csatlós [d], L. Csige [d], B. Davids [a], U. Garg [e], J. Gulyás [d], M.N. Harakeh [a], M.A. de Huu [a], B.C. Junk [c], A. Krasznahorkay [d], S. Rakers [c], D. Sohler [d], H.J. Wörtche [a]

[a] *Kernfysisch Versneller Instituut, 9747 AA Groningen, The Netherlands*
[b] *INFN, Milano, I-20133 Milano, Italy*
[c] *Westfälische Wilhelms-Universität, Münster D-48149, Germany*
[d] *Institute of Nuclear Research of the Hungarian Academy of Sciences, H-4001 Debrecen, Hungary*
[e] *University of Notre Dame, Notre Dame, IN 46556, USA*

Received 24 September 2003; accepted 6 October 2003

Editor: V. Metag

Abstract

The direct proton decay of the isoscalar giant dipole resonance (ISGDR) has been studied in ^{208}Pb using the $(\alpha, \alpha' p)$ reaction at a bombarding energy of 200 MeV. Through observation of direct-decay protons from the ISGDR in coincidence with scattered α-particles, the population of proton–hole states in ^{207}Tl was studied, allowing us to test recently performed continuum-RPA (CRPA) calculations for the ISGDR and thereby to learn about its microscopic structure. The energy and width of the ISGDR were also determined to be 22.1 ± 0.3 MeV and 3.8 ± 0.8 MeV, respectively. A new resonance of quadrupole character was observed at $E_x = 26.9 \pm 0.7$ MeV with a width of 6.0 ± 1.3 MeV.

PACS: 24.30.Cz; 25.55.Ci; 27.80.+w

Of all the giant resonances investigated so far, the isoscalar giant dipole resonance (ISGDR) has remained one of the most interesting collective vibrational modes of nuclei. The first-order term of the isoscalar dipole transition operator is associated with a spurious center-of-mass motion, and only the higher-order terms lead to intrinsic excitation of the nucleus. Microscopically, the ISGDR is described as coherent $1\hbar\omega$ and $3\hbar\omega$ particle–hole excitations with most of the strength concentrated in the $3\hbar\omega$ component [1]. Macroscopically, the ISGDR can be described as a density oscillation (squeezing mode), whose oscillator frequency is determined by the compression modulus of the nucleus [2,3]. As a consequence, the excitation energy of the ISGDR can directly be related to the nuclear incompressibility, a key term of the nuclear equation-of-state [3]. Therefore, the study of the ISGDR offers an alternative and complementary method to the systematic studies of the nuclear incompressibility based on the isoscalar giant monopole resonance (ISGMR) [4,5].

E-mail address: hunyadi@atomki.hu (M. Hunyadi).

[1] On leave from the Institute of Nuclear Research of the Hungarian Academy of Sciences, Debrecen, Hungary.

0370-2693/$ – see front matter © 2003 Published by Elsevier B.V.
doi:10.1016/j.physletb.2003.10.016

The primary goal of the earlier studies in singles measurements of the ISGDR was to find unambiguous evidence for the presence of the $3\hbar\omega$ isoscalar dipole strength in a few medium-heavy and heavy nuclei [6–11]. One way to identify the ISGDR in singles experiments is the measurement of angular distributions at very forward angles, where differences in the shapes of the angular distributions can help to disentangle strengths with different multipolarities. On the other hand, experiments performed very close to 0° often suffer from a substantial contribution from instrumental background in addition to the underlying nuclear continuum [6–11]. The first unambiguous results on the excitation energy of the ISGDR were reported only in recent years by measurements applying the difference-of-spectra method at very forward angles [9], or multipole decomposition techniques in a wide angular range [10,11].

In this Letter, we report the first investigation of direct-proton decay of the ISGDR in ^{208}Pb, using inelastic α-scattering at a beam energy of 200 MeV [12]. The experimental goal of our coincidence measurement was to deduce partial decay branching ratios of the ISGDR to various final states in ^{207}Tl in order to allow a comparison with the results of recent CRPA calculations [13,14]. These calculations predicted significant decay widths from the ISGDR to some proton–hole states in ^{207}Tl. In the decay measurements, these proton–hole states are predominantly populated via the direct-decay channels, which are connected to the partial escape widths of the ISGDR. Furthermore, the application of coincidence techniques helps to suppress the instrumental background. Considerable suppression of the nuclear continuum is provided when the coincidence detectors are placed at large angles with respect to the beam axis, which effectively removes the contributions of quasi-free processes like pickup-breakup or knockout reactions, which are forward peaked. Since the ISGDR lies well above the proton-decay threshold and Coulomb barrier, this has the potential of allowing a better determination of the excitation energy and total width of the ISGDR because of the much cleaner background situation.

The experiment was performed at the AGOR superconducting cyclotron facility of the KVI, using the ^{208}Pb$(\alpha,\alpha' p)$ reaction at a beam energy of 200 MeV incident on an enriched (97%) ^{208}Pb target with a thickness of 3.5 mg/cm^2. The scattered α-particles were detected by the EuroSuperNova detector system [15] installed at the focal plane of the Big-Bite Spectrometer (BBS) [16]. The BBS enables the detection of ejectiles with a wide momentum acceptance, corresponding to an excitation energy range of 3–70 MeV in the present setup, and with an angular acceptance of 1.5°–6.0°, covering a solid angle of 6 msr. The protons were detected by a detector-ball with a radius of 10 cm consisting of 16 5-mm thick Si(Li)-detectors mounted in the backward hemisphere of the scattering chamber, covering 100°–220° in the laboratory frame. The solid angle subtended by the Si(Li)-detector ball was 1 sr. The energy calibrations of the focal plane and the Si(Li)-detectors were provided by measurements on Ta_2O_5 and ^{12}C targets using (α,α') and $(\alpha,\alpha' p)$ reactions. The resolutions in the excitation energy of ^{208}Pb* parent and ^{207}Tl* daughter nuclei were 400 and 600 keV full width at half maximum (FWHM), respectively.

A strong contribution to the coincidence background is present due to the oxygen contamination of the target. The pulse-shape discrimination capabilities of the Si(Li)-detectors [17] were used to identify α-particles and protons originating from excited ^{208}Pb and ^{16}O target nuclei. The proton-decay events to the hole states in ^{207}Tl are well separated from those to hole states in ^{15}N due to the different proton emission thresholds of the parent nuclei: $S_p(^{16}\text{O}) = 12.127$ MeV, $S_p(^{208}\text{Pb}) = 8.008$ MeV.

The population of four of the proton–hole states ($3s_{1/2}$, $2d_{3/2}$, $1h_{11/2}$, $2d_{5/2}$) [18] was observed as loci in the 2-dimensional plot (see Fig. 1) of the proton energy E_p versus the excitation energy E_x in ^{208}Pb. After correcting the prompt events for random coincidences, the loci were projected onto the final-state energy axis. A projection of the E_{fs}-spectrum gated on the ISGDR region is shown in Fig. 2. The overall resolution of the final-state energy of 600 keV (FWHM) did not allow the separation of the close-lying hole states, but resulted in two enhanced structures (denoted as groups A and B), one comprising the $3s_{1/2}$, $2d_{3/2}$ hole states and the other comprising the $1h_{11/2}$, $2d_{5/2}$ hole states, respectively. In addition, a weak structure at the location of the $1g_{7/2}$ hole state is observed. The observation that the $1h_{11/2}$ hole state is weakly populated compared to the $2d_{5/2}$ hole state in group B can be explained qualitatively by the lower transmission probability due to

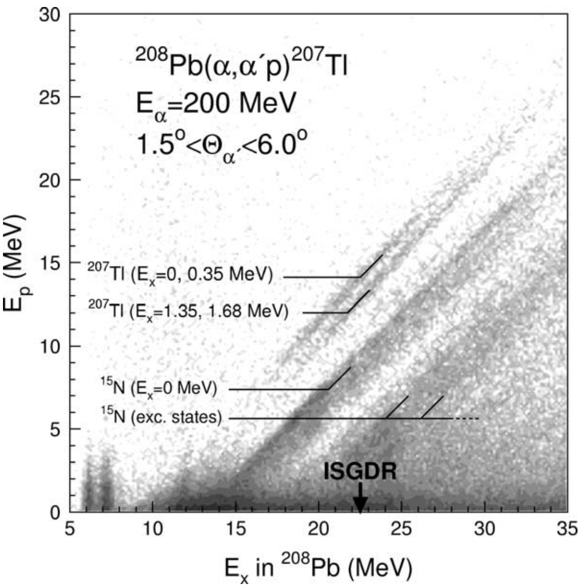

Fig. 1. 2-dimensional plot of the decay-proton energy E_p versus the excitation energy E_x in ^{208}Pb. The loci for the final states in ^{207}Tl and ^{15}N populated by the decay from ^{208}Pb and the oxygen contaminant, respectively, are also indicated.

the higher centrifugal barrier of the single-particle decay.

In order to deduce the partial double-differential cross sections, $d^2\sigma/d\Omega_{\alpha'}\,dE_{\alpha'}$, for the decay channels to the hole states in ^{207}Tl, an assumption for the angular correlation function of the protons had to be made. The experimental angular correlations were generated knowing the positions of the proton-detectors and the recoil axis of the excited ^{208}Pb* nuclei, and were fitted with polynomials up to fourth order. The obtained fit-functions for the triple-differential cross sections, $d^3\sigma/d\Omega_{\alpha'}\,dE_{\alpha'}\,d\Omega_p$, were integrated over 4π, yielding the double-differential cross sections. The whole procedure was repeated applying gates on each excitation-energy bin of 1 MeV, and on the final-state groups A and B, except for the $1g_{7/2}$ hole state, which was left out from the analysis due to its poor statistics. The double-differential cross sections are shown in Fig. 3 as a function of the excitation energy in ^{208}Pb. The spectra were also gated on the scattering-angle region of $\Theta_{\mathrm{c.m.}} = 1.5°$–$3.0°$, where the theoretical angular distribution of the inelastic α-scattering predicts a maximum for the ISGDR population cross section around 1.8°.

In both proton-coincidence spectra the ISGDR can easily be recognized as a well-pronounced structure showing significant decay cross sections to both final-state groups in ^{207}Tl. The effect of the Coulomb and centrifugal barriers on the decay cross sections close to the barrier is maximum around $E_x = 18$ MeV. It reduces the observed strength of the HEOR and shifts its centroid up-wards in excitation energy, while its influence on the ISGDR distribution is rather weak. This picture holds only if the centrifugal barrier is

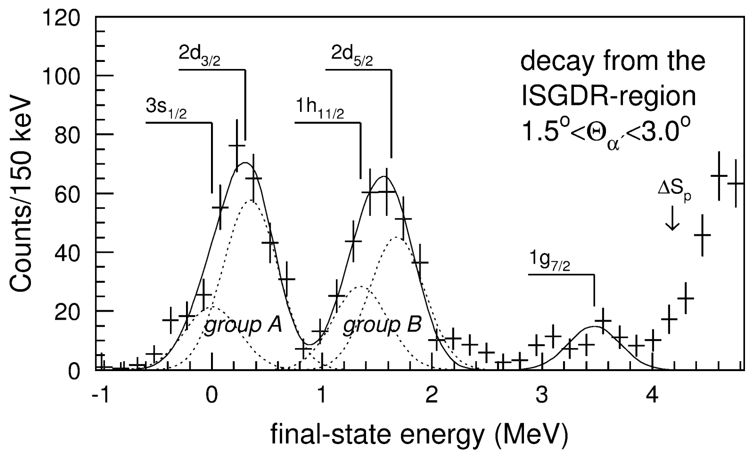

Fig. 2. The final-state spectrum of the low-lying proton–hole states in ^{207}Tl generated by gating on the ISGDR region, and on scattering angles of $\Theta_{\mathrm{c.m.}} = 1.5°$–$3.0°$. The locations and the fits of the important hole states are also shown. $\Delta S_p = S_p(^{16}\mathrm{O}) - S_p(^{208}\mathrm{Pb})$ indicates the proton-emission threshold of ^{16}O in the E_{fs}-scale of ^{207}Tl.

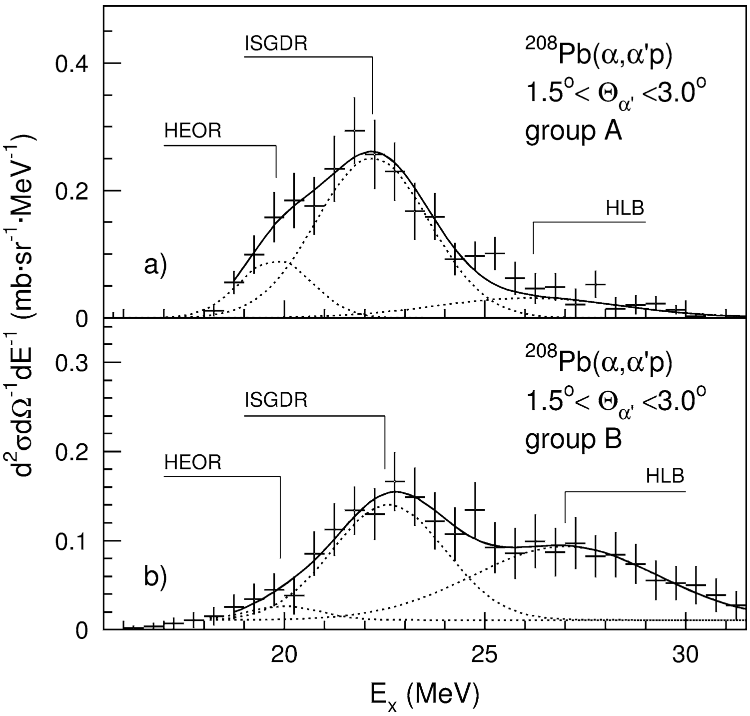

Fig. 3. Double-differential cross sections as a function of the excitation energy gated on the indicated scattering angles and measured in coincidence with direct-decay protons of (a) group A and (b) group B. The fits of the HEOR, ISGDR and the higher-lying bump (HLB) are also shown.

not significant with respect to the Coulomb barrier, as may be assumed in the case of proton-decay channels with low angular momentum l. Indeed, the ISGDR decay populates the $3s_{1/2}$, $2d_{3/2}$ and $2d_{5/2}$ final-states in ^{207}Tl through p-wave protons, whereas the weak population of the $1h_{11/2}$ hole state can be ascribed to the associated $l = 4$ single-particle decay.

In the case of the underlying continuum background, the more complex and generally unknown multipole composition would favor statistical decay mainly proceeding via neutron emission but direct-proton decay could be possible for collective multipole strength distributed widely in excitation energy. The latter could be the reason for the enhanced continuum contribution for decay channels to the final-state group B, which comprises higher angular momentum final states than group A. The bump observed at higher excitation energy in coincidence with proton decay to final-state group B could have multipolarity $L \geqslant 2$ as we will discuss below.

The ISGDR strength was determined by integrating the double-differential cross section over the region of $E_x = 19$–25 MeV after subtracting the contributions of the fitted lower-lying HEOR and higher-lying bump. The angular distributions of the ISGDR strength were deduced by plotting the obtained differential cross sections as a function of scattering angle. A similar analysis was performed for the angular distributions of the high-lying broad bump applying the same integration procedure over the region of $E_x = 25$–31 MeV. The results are shown in Fig. 4. The experimental differential cross sections as a function of the scattering angle were compared to theoretical calculations performed within the framework of the distorted-wave Born-approximation (DWBA) using the code CHUCK [19]. The optical-model parameters were adopted from Ref. [20] and the form factor for the ISGDR from Ref. [2]. For $L \geqslant 2$, the form factors were of the usual, first-derivative type. A χ^2-analysis of the fits for the ISGDR unambiguously confirmed the $L = 1$ character in both decay-

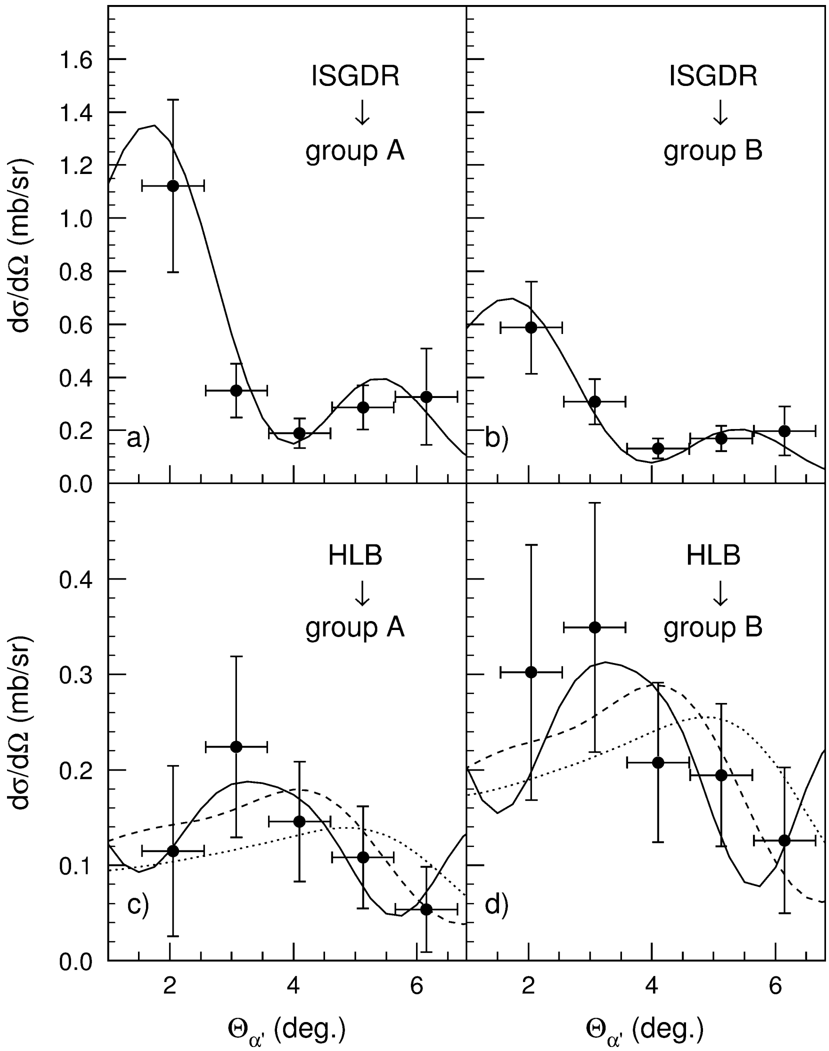

Fig. 4. Differential cross sections of the ISGDR and the continuum above $E_x > 25$ MeV gated on the direct-decay protons of both final-state groups. The theoretical angular distributions for various multipole transitions obtained from a χ^2-analysis are compared to the experimental data. The solid curves represent $L = 1$ transitions in panels (a) and (b), $L = 2$ in panels (c) and (d). The dashed and dotted curves represent the $L = 3$ and $L = 4$ transitions, respectively, in panels (c) and (d).

branches (see Fig. 4(a), (b)). For the bump above the ISGDR in excitation energy, the χ^2-analysis resulted in an $L = 2$ multipolarity with the highest confidence level; however, an $L = 3$ assignment was also within the limits of acceptability (see Fig. 4(c), (d)). A transition with $L \geqslant 2$ for the bump may also explain the increased population of group B ($1h_{11/2}$, $2d_{5/2}$ hole states) from excitation energies $E_x > 25$ MeV, because of a lower angular momentum for proton decay and therefore higher transmission probabilities of decay to the $1h_{11/2}$ hole state. The higher-lying bump may be explained as the excitation of the overtone of the isoscalar quadrupole resonance (ISGQR), i.e., the response to the second-order quadrupole operator.

The partial differential cross sections of the decay channels from the ISGDR in ^{208}Pb to the hole states in ^{207}Tl are expressed in terms of the energy-weighted sum rule (EWSR) and compared to the results of the CRPA-calculations in Table 1. While the theoretical and experimental values for the decay branch to group

Table 1
Experimental partial differential cross sections for direct-proton decay of the ISGDR in ^{208}Pb to proton–hole states in ^{207}Tl, expressed in percentages of the EWSR. The theoretical branching ratios b_i, which refer to the total strength of the ISGDR, were also normalized to the EWSR using an exhaustion fraction of $S = 76\%$ taken from the CRPA-calculations of Ref. [13]

Final state	E_{fs} (MeV)	$d\sigma_{exp}/d\Omega^a$ (EWSR)	$b_i \cdot S^b$ (EWSR)
$3s_{1/2}$	0	$3.1 \pm 1.1\%$ (group A)	0.18%
$2d_{3/2}$	0.35		0.46%
$1h_{11/2}$	1.35	$1.6 \pm 0.6\%$ (group B)	–
$2d_{5/2}$	1.68		1.09%

[a] This work.
[b] Ref. [13].

B show a rather satisfactory agreement, the comparison for those to group A results indicates a deviation with a factor of approximately 5. This finding can also be expressed as the comparison of the experimentally determined ratio of population cross sections $(d\sigma_A/d\Omega)/(d\sigma_B/d\Omega) = 1.94 \pm 1.00$ to the ratio of the theoretical branching ratios $b_A/b_B = 0.59$. Since the systematic errors of the experimental observables and uncertainties in the calculation of the EWSR and exhaustion fractions cancel out by taking the ratios, the relative branching ratios can provide more sensitive and reliable tests of the microscopic parameters of the CRPA-calculations, e.g., assumptions on the continuum coupling and the doorway-state resonances.

As mentioned above, the shape of the resonances can be modified by the changing transmission probability as a function of the excitation energy since the energy of the protons emitted from the region of the ISGDR is near the top of the Coulomb and centrifugal barriers. Furthermore, the cross section per unit strength changes as a function of the excitation energy. These two effects may distort the shapes of the resonances to be studied and could possibly lead to an incorrect determination of the excitation energy (E_x) and width (Γ) of the resonances using the (α, α') or $(\alpha, \alpha' p)$ data. Therefore, the shapes of the HEOR and the ISGDR distributions, corrected for the transmission probabilities and the E_x-dependence of the inelastic scattering cross sections, were determined by calculations using centroid energies taken from Refs. [9,11], and appeared to be slightly shifted up in E_x, but preserving the assumed Gaussian shapes. To obtain the proper energy and width of the ISGDR these effects were deconvoluted. The fitted centroid energy of the ISGDR, after proper deconvolution of transmission probabilities and E_x-dependence of the excitation cross section, was $E_x = 22.1 \pm 0.3$ MeV, and the fitted width was $\Gamma = 3.8 \pm 0.8$ MeV. These results were compared to the systematics of the ISGDR excitation energy and width. Remarkable agreement has been obtained with the experimental values of Ref. [9] and theoretical values of Ref. [13]. The agreement with the results obtained by the multipole-decomposition analysis of Refs. [10,11] is not as good. Although the excitation energy for the ISGDR obtained by Uchida et al. (Fig. 3(b) of Ref. [11]) without subtracting any underlying continuum agrees with ours, the width is much larger than any result obtained by others, raising questions about the nature of the nuclear continuum included in their ISGDR fit but not observed in our coincidence data. On the other hand, the lower excitation energy obtained by Ref. [10] may result from an overestimation of the nuclear continuum subtracted. Our present result for the excitation energy of the ISGDR confirms the results of the latest studies probing the consistency of nuclear incompressibilities from ISGMR and ISGDR excitation energies (see Ref. [11] and references therein). The excitation energy and width of the "$L = 2$" bump was $E_x = 26.9 \pm 0.7$ MeV and $\Gamma = 6.0 \pm 1.3$ MeV.

In conclusion, we have performed the first coincidence experiment to investigate the direct proton decay channels of the ISGDR using the ^{208}Pb$(\alpha, \alpha' p)$ reaction at $E_\alpha = 200$ MeV. The double-differential cross sections determined for the ISGDR and a newly observed bump at higher excitation energy were analyzed by fitting to DWBA calculations, confirming the $L = 1$ character of the first and favoring an $L = 2$ character for the second. If the quadrupole character for this mode (overtone of the ISGQR) is confirmed it would correspond to the first observation of the third compressional mode next to the ISGMR and ISGDR. The differential cross sections were deduced for decay of the ISGDR to low-lying proton–hole states in ^{207}Tl, and were compared to microscopic calculations based on CRPA theory. The agreement is far from perfect requiring a new look at these calculations (see in this connection Ref. [21]). The result obtained for the excitation energy strengthens the argument regarding the consistency of the nuclear incompressibility derived from ISGMR and ISGDR systematics.

Acknowledgements

We acknowledge the European Commission support in the frameworks of the Marie Curie Fellowship program under contract HPMF-CT-2000-00663 and transnational access program under contract HPRI-CT-1999-00109. This work was performed as a part of the research program of the Dutch Stichting FOM with financial support from the Dutch NWO. The Hungarian co-authors acknowledge the Hungarian fund OTKA under contracts N32570, D34587 and T038404. U. Garg acknowledges a grant from the US National Science Foundation (number PHY-0140324).

References

[1] T.D. Poelhekken, et al., Phys. Lett. B 278 (1992) 423.
[2] M.N. Harakeh, A.E.L. Dieperink, Phys. Rev. C 23 (1981) 2329; M.N. Harakeh, Phys. Lett. B 90 (1980) 13.
[3] S. Stringari, Phys. Lett. B 108 (1982) 232.
[4] M.N. Harakeh, et al., Phys. Rev. Lett. 38 (1977) 676.
[5] D.H. Youngblood, et al., Phys. Rev. Lett. 82 (1999) 691, and references therein.
[6] C. Djalali, et al., Nucl. Phys. A 380 (1982) 42.
[7] H.P. Morsch, et al., Phys. Rev. Lett. 45 (1980) 337; H.P. Morsch, et al., Phys. Rev. C 28 (1983) 1947.
[8] G.S. Adams, et al., Phys. Rev. C 33 (1986) 2054.
[9] B.F. Davis, et al., Phys. Rev. Lett. 79 (1997) 609.
[10] H.L. Clark, Y.-W. Lui, D.H. Youngblood, Phys. Rev. C 63 (2001) 031301(R).
[11] M. Uchida, et al., Phys. Lett. B 557 (2003) 12.
[12] A similar measurement has been done at 400 MeV recently. B.K. Nayak, et al., private communication.
[13] M.L. Gorelik, et al., Phys. Rev. C 62 (2000) 044301.
[14] M.L. Gorelik, M.H. Urin, Phys. Rev. C 64 (2001) 047301.
[15] H.J. Wörtche, Nucl. Phys. A 687 (2001) 321c.
[16] A.M. van den Berg, Nucl. Instrum. Methods B 99 (1995) 637.
[17] G. Pausch, et al., Nucl. Instrum. Methods A 365 (1995) 176.
[18] M.J. Martin, Nucl. Data Sheets 70 (1993) 315.
[19] P.D. Kunz, University of Colorado, 1983, unpublished.
[20] L. Bimbot, et al., Nucl. Phys. A 210 (1973) 397.
[21] M.L. Gorelik, M.H. Urin, nucl-th/0209094.